Cell Communication and Signaling

RESEARCH

Open Access

MDA5 protein mediating persistent ER stress/unfolded protein response contributes to endothelial-mesenchymal-transition of lung microvascular endothelial cell in dermatomyositis

Li-Qin Zhao[1], Xue-Qing Yang[1], Qian Niu[1], Xiao Feng[2], He-De Zhang[2], Shu-Yi Ye[1], Li-Juan Jiang[3], Fan Yu[1,4], Hong Ye[2,4,6*] and Wan-Li Ma[1,4,5*]

Abstract

Background Dermatomyositis (DM) is an idiopathic inflammatory myopathy. Anti-MDA5 antibody positive DM (MDA5 + DM) is a distinct subtype of the disease. The model of anti-MDA5 antibody positive DM has been already reported. However, the detailed role and mechanism of MDA5 in vascular damage was still poorly understood.

Methods Clinical information was retrospectively collected, and a total of 127 DM patients were enrolled. Serum from DM patients and control subjects was used to treat mouse lung microvascular endothelial cells (MVECs) to investigate vascular changes. Western blotting, quantitative real-time polymerase chain reaction (qRT-PCR), immunofluorescence staining, immunoprecipitation, protein mass spectrometry, flow cytometry and bioinformatics analysis were used.

Results Firstly, clinical data analysis revealed that vascular damage and interstitial lung disease (ILD) was correlated with anti-MDA5 antibody in DM patients. Then, serum from patients was used to treat mouse lung MVECs. Serum from MDA5 + DM patients induced endothelial-mesenchymal-transition (EndMT) in MVECs, and the EndMT in MVECs was mediated by TRB3/ERK/Snai-1 pathway. Next, increased-TRB3 was confirmed induced by persistent ER stress/unfolded protein response (UPR). Notably, persistent ER stress/UPR resulted from MDA5 protein binding with PERK. At last, T cell-derived IFN-β was found to induce MDA5 expression in DM patients.

Conclusion MDA5 protein mediating persistent ER stress/UPR contributed to EndMT in vascular endothelial cells, which should be involved in MDA5 + DM related ILD.

*Correspondence:
Hong Ye
yehmwl@hust.edu.cn
Wan-Li Ma
whmawl@hust.edu.cn

Full list of author information is available at the end of the article

© The Author(s) 2025. **Open Access** This article is licensed under a Creative Commons Attribution-NonCommercial-NoDerivatives 4.0 International License, which permits any non-commercial use, sharing, distribution and reproduction in any medium or format, as long as you give appropriate credit to the original author(s) and the source, provide a link to the Creative Commons licence, and indicate if you modified the licensed material. You do not have permission under this licence to share adapted material derived from this article or parts of it. The images or other third party material in this article are included in the article's Creative Commons licence, unless indicated otherwise in a credit line to the material. If material is not included in the article's Creative Commons licence and your intended use is not permitted by statutory regulation or exceeds the permitted use, you will need to obtain permission directly from the copyright holder. To view a copy of this licence, visit http://creativecommons.org/licenses/by-nc-nd/4.0/.

Keywords MDA5, Anti-MDA5 antibody, Dermatomyositis (DM), Interstitial lung disease (ILD), Endothelial-Mesenchymal-Transition (EndMT), Endoplasmic reticulum stress (ER stress), Unfolded protein responses (UPR)

Background

Dermatomyositis (DM) is one of idiopathic inflammatory myopathy which is a group of diseases including polymyositis, inclusion body myositis, immune-mediated necrotizing myopathy and overlap myositis [1]. DM is characterized by skin changes and muscle weakness. The prevalence of DM is about 20 per 100,000 people, and the incidence is 5 ~ 10 per 100,000 people per year [2, 3]. Auto-antibodies in idiopathic inflammatory myopathy are divided into myositis-specific antibodies and myositis-associated antibodies. Antibody against to melanoma differentiation-associated gene 5 protein (MDA5) belongs to myositis-specific antibodies. Half of DM patients are positive of anti-MDA5 antibodies in Chinese patients with DM [4]. Interstitial lung disease (ILD) is a severe DM-related disease. Once DM patient got ILD, the severity of disease will increase, and the quality of life will decrease. The incidence of ILD was higher in anti-MDA5 antibody positive DM (MDA5 + DM) patients than anti-MDA5 antibody negative DM (MDA5- DM) patients [5].

MDA5 + DM patients were significantly more likely to have vasculopathy than MDA5- DM patients [6]. Vasculopathy characterized by vascular fibrin deposition with variable perivascular inflammation [7]. Shakshouk H and colleagues compared the skin biopsies of MDA5 + DM patients and those from MDA5- DM patients, there was no statistically significant difference in any of the histopathological findings except for vasculopathy [8]. *MDA5* is one of the retinoic acid-inducible gene I-like receptor genes. MDA5 proteins express and localize in the cytoplasm when the cells recognize long dsRNA or self-aberrant dsRNA [9, 10]. Recognizing self-RNA is thought to be the reason of MDA5 abnormal activation in autoimmune diseases [11]. The biological functions of MDA5 were mainly mediating inflammatory responses [12]. The expression of MDA5 protein was difference in different cells. Poly (I: C)-induced MDA5 is higher in endothelial cells and fibroblasts than epithelial cells [13]. MDA5 has higher expression in lung and skin tissues than in muscle tissues in DM patients [14, 15]. The mouse model of anti-MDA5 antibody positive DM has been already reported [16]. However, the detailed role and mechanism of MDA5 in vasculopathy was still poorly understood.

The endoplasmic reticulum (ER) is an organelle responsible for maintaining calcium homeostasis, cholesterol production, lipid synthesis, and synthesizing and folding proteins. Any abnormality in these biological processes can disrupt ER homeostasis, that's called ER stress [17]. In response to perturbations, ER-associated degradation removes aberrant protein productions. The unfolded protein response (UPR) followed ER stress regulates transcription and translation depending on the stress intensity, UPR induces cell adaptive changes or promotes apoptosis [17, 18]. UPR includes three signal pathways: the inositol-requiring enzyme 1 (IRE1α) pathway, protein kinase RNA-like ER kinase (PERK) pathway, and ER-membrane-associated activating transcription factor 6 (ATF6) pathway [19]. The PERK pathway is associated with adaptive cellular changes in fibrosis and apoptosis. Tribbles homolog 3 (TRB3) is the key protein in crosstalk between PERK pathway and other signaling pathway regarding innate immunity, metabolism and cell fate. Studies reported that ER stress existed in DM patients. However, it was unknown whether ER stress and subsequent signaling pathways were involved in vascular damage in DM.

In this study, multidisciplinary approaches were employed including integrating clinical data analysis, bioinformatics and experimental techniques to elucidate role and the underlying mechanism of MDA5 protein in vascular damage of DM.

Results

Vascular damage and ILD was correlated with anti-MDA5 antibody in DM patients

The clinical information was retrospectively collected, and a total of 127 DM patients were enrolled (Fig. S1A). The baseline characteristics of patients with anti-MDA5 antibody positive (MDA5 + DM) and anti-MDA5 antibody negative (MDA5- DM) were shown in Table S1. MDA5 + DM patients were 90.6% with ILD, and MDA5- DM were 59.7% (Table S1). The disease activity score (DAS) skin score of DM was higher in MDA5 + DM than that in MDA5- DM patients (Table S1 and Fig. S1B). At the same time, multivariable logistic analyses showed that ILD (OR 4.440, $P = 0.046$) and DAS skin score (OR 1.842, $P = 0.021$) was correlated with positive of anti-MDA5 antibody in DM patients (Table S2).

The DAS skin score is a score for skin lesions. Researchers found that the DAS skin score associated with vascular damage [20, 21]. It was reported that vasculopathy was the only histopathological finding in skin biopsies that has statistical significance between MDA5 + DM and MDA5- DM [8]. Therefore, changes of lung vascular endothelial cells in MDA5 + DM microenvironment as well as the underlying mechanism were investigated.

Serum from MDA5 + DM patients induced EndMT in MVECs

Endothelial-mesenchymal-transition (EndMT) is a one of important mechanisms after cell damage in the process

of diseases including ILD. To understand changes of lung vascular endothelial cells, EndMT in the cells was investigated. Mouse lung microvascular endothelial cells (MVECs) were isolated by magnetic sorting and identified (Fig. S2). Then, serum from DM patient and control subject was used to treat these MVECs. Clinical information of subjects whose blood was collected was shown in Table S3 and Table S4. As shown in Fig. 1A-C, compared with serum from MDA5- DM and control subject, serum from MDA5 + DM induced increases of protein collagen-I, fibronectin and vimentin, but decreased endothelial marker CD31. Serum from MDA5 + DM also mediated MVEC cell viability (Fig. 1D). Moreover, immunofluorescence staining also showed increased vimentin protein and decreased CD31 protein in MDA5 + DM serum treated cells (Fig. 1E and F). To further confirmed the role of MDA5 + DM serum in EndMT, mouse lung MVECs were treated with a serial concentration MDA5 + DM serum (0, 5, 10, 20%). MDA5 + DM serum induced concentration-dependent changes of collagen-I, fibronectin, vimentin, and CD31 protein (Fig. S3). Moreover, human lung MVECs were also used. As shown in Fig. S4, serum from MDA5 + DM patients induced EndMT in human lung MVECs too. These results indicated that serum from MDA5 + DM induced EndMT in MVECs.

MAPK-ERK/Snai-1 signaling was involved in EndMT of MVECs

Snai-1 is a key transcription factor in EndMT. To investigate mechanism of EndMT in MVECs, Snai-1 protein

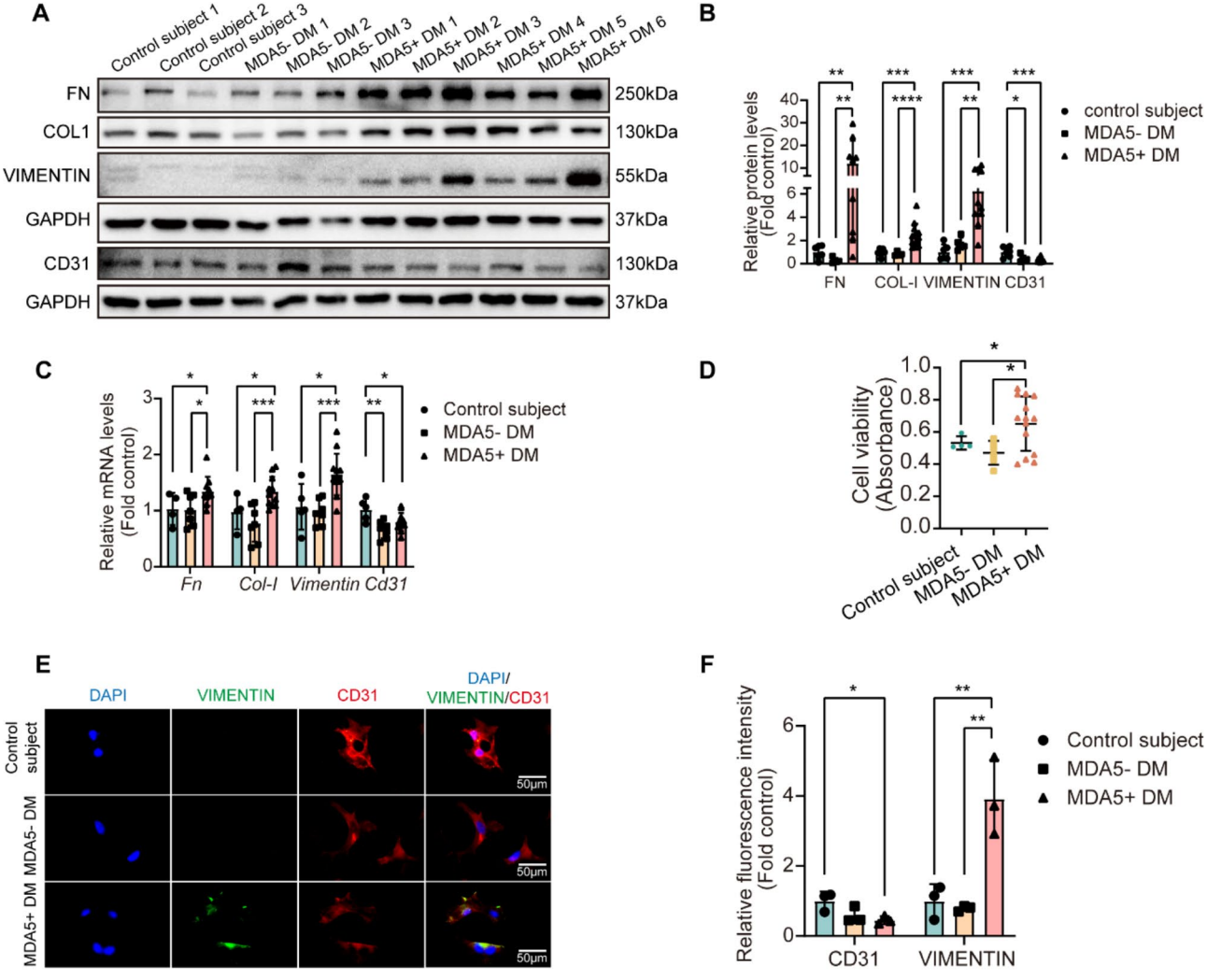

Fig. 1 Sera from MDA5 + DM patients induced EndMT in primary mouse lung microvascular endothelial cells. Primary mouse lung microvascular endothelial cells (MVECs) were treated with 10% serum from control subjects, MDA5- DM patients and MDA5 + DM patients. (**A**, **B**) MVECs were treated with serum for 48 h, after which protein levels of fibronectin (FN), collagen I (COL-I), vimentin and CD31 were measured by western blotting. $n = 6 \sim 12$. (**C**) Cells were treated with serum for 21 h, mRNA levels were measured by qRT-PCR. $n = 5 \sim 12$. (**D**, **E**) Cells were treated with serum for 48 h. Cell viability was assayed by CCK8 (**D**). $n = 4 \sim 14$. Immunofluorescence staining was performed to show protein expressions of vimentin and CD31 (**E** and **F**). *P* values were calculated using One-way ANOVA followed by Bonferroni's test. $^{*}P < 0.05$, $^{**}P < 0.01$, $^{***}P < 0.001$, $^{****}P < 0.0001$

was detected. As shown in Fig. 2A-C, MDA5 + DM serum increased Snai-1 protein and mRNA level in primary mouse MVECs. Snai-1 is mainly regulated by MAPK, PI3K, and SMAD/TGF-β pathway. Compared with serum from MDA5- DM and control subjects, the serum from MDA5 + DM did not activate or slight decreased SMAD, PI3K and p65 signaling in MVECs (Fig. S5). Notably, as a MAPK signaling, p-ERK was obviously increased in MDA5 + DM serum treated-MVECs (Fig. 2D and E). These data revealed that MAPK-ERK/Snai-1 pathway was involved in MDA5 + DM serum-induced EndMT.

TRB3 phosphorylated ERK in MVECs

To find proteins which phosphorylate ERK, protein kinases of ERK were screened on the PhosphoSitePlus website. At the same time, studies have suggested that TRB3 cross-talks with ERK by phosphorylating ERK [22, 23]. Based on these data, ERK related proteins were visualized by the String website (Fig. S6A). MEK, EGFR and TRB3 were found upregulation in MVECs which treated with MDA5 + DM serum compared with control subject or MDA5- DM serum (Fig. S6B-D, Fig. 3A and B). Firstly, MEK specific inhibitor AZD8330 was used to inhibit MEK enzyme activity. As shown in Fig. S4E and F, AZD8330 even a high concentration dose did not prevent phosphorylation of ERK. EGFR inhibitor BIBW2992 failed to inhibit phosphorylation of ERK either (Fig. S6G and H). Therefore, that's TRB3 which maybe phosphorylate ERK.

TRB3 is a member of the unfolded protein response (UPR)-PERK signaling pathway, which links ER stress/UPR to other signal pathways. Thus, the role of TRB3 in ERK activation should be examined in MVECs. As shown in Fig. 3A and B, MDA5 + DM serum increased TRB3 expression in MVECs treated by MDA5 + DM serum. Co-IP showed that TRB3 interacted with ERK (Fig. 3C). Then, TRB3 siRNA was designed and conformed to inhibit expression of TRB3 protein induced by MDA5 + DM serum (Fig. S7). As shown in Fig. 3D-K, MDA5 + DM serum induced increases of p-ERK and EndMT in MVECs, but these were prevented by TRB3 siRNA.

However, it was completely opposite to MDA5 + DM serum treated cells, an interesting phenomenon was found in MDA5- DM serum treated cells. As shown in Fig. 3G and H, TRB3 siRNA increased p-ERK in MDA5- DM serum treated-MVECs. To confirm this contradictory result, EndMT was detected in TRB3 siRNA- and MDA5- DM serum-treated cells. As shown in Fig. S8, TRB3 siRNA certainly increased p-ERK, and induced EndMT in MDA5- DM serum treated-MVECs. Thus, it was raised a presumption that TRB3 should

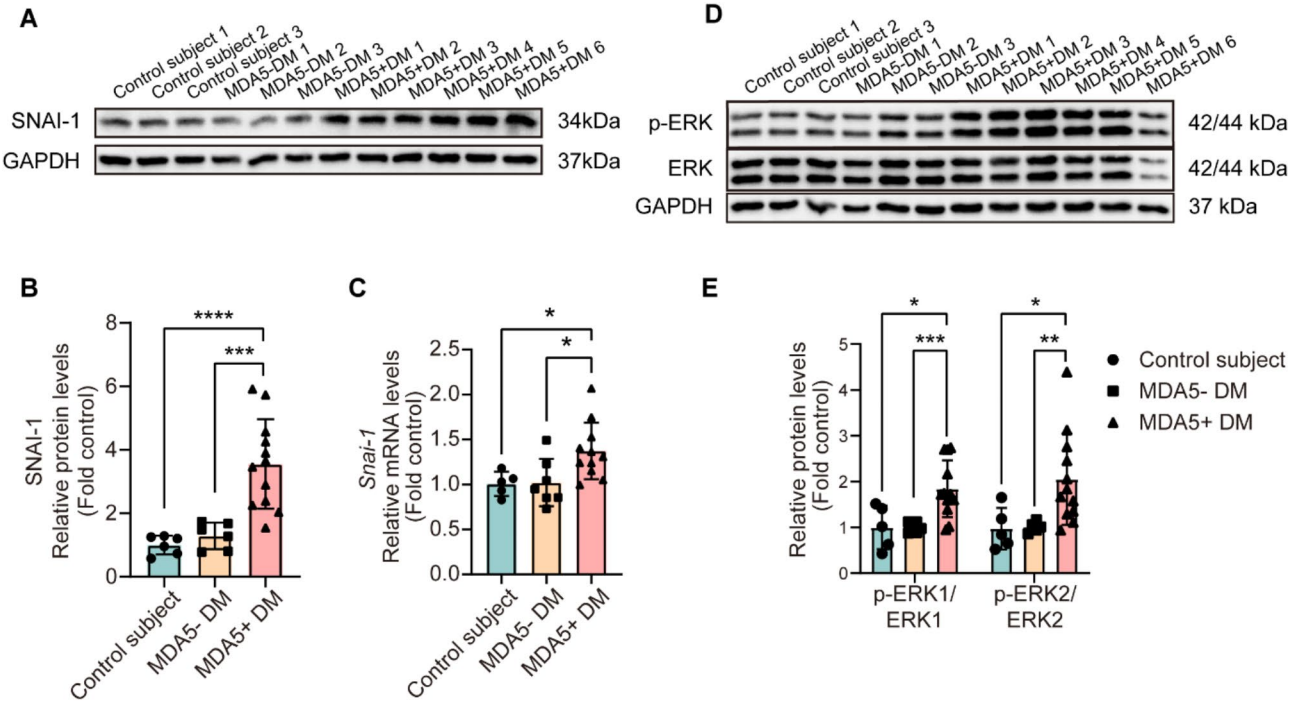

Fig. 2 Serum from MDA5 + DM patients up-regulated transcription factor Snai-1 and increased ERK phosphorylation. Primary mouse lung MVECs were treated with serum (10%) from control subjects, MDA5- DM and MDA5 + DM patients. (**A**, **B**, **D**, **E**) Cells were treated with serum for 48 h, after which protein levels of SNAI-1, p-ERK/ERK were measured by Western blotting. (**C**) Cells were treated with serum for 21 h, mRNA levels of *Snai-1* were detected by qRT-PCR. Control subjects, $n = 6$; MDA5- DM patients, $n = 6$; MDA5 + DM patients, $n = 11$. *P* values were calculated using One-way ANOVA followed by Bonferroni's test. $^{*}P < 0.05$, $^{**}P < 0.01$, $^{***}P < 0.001$, $^{****}P < 0.0001$

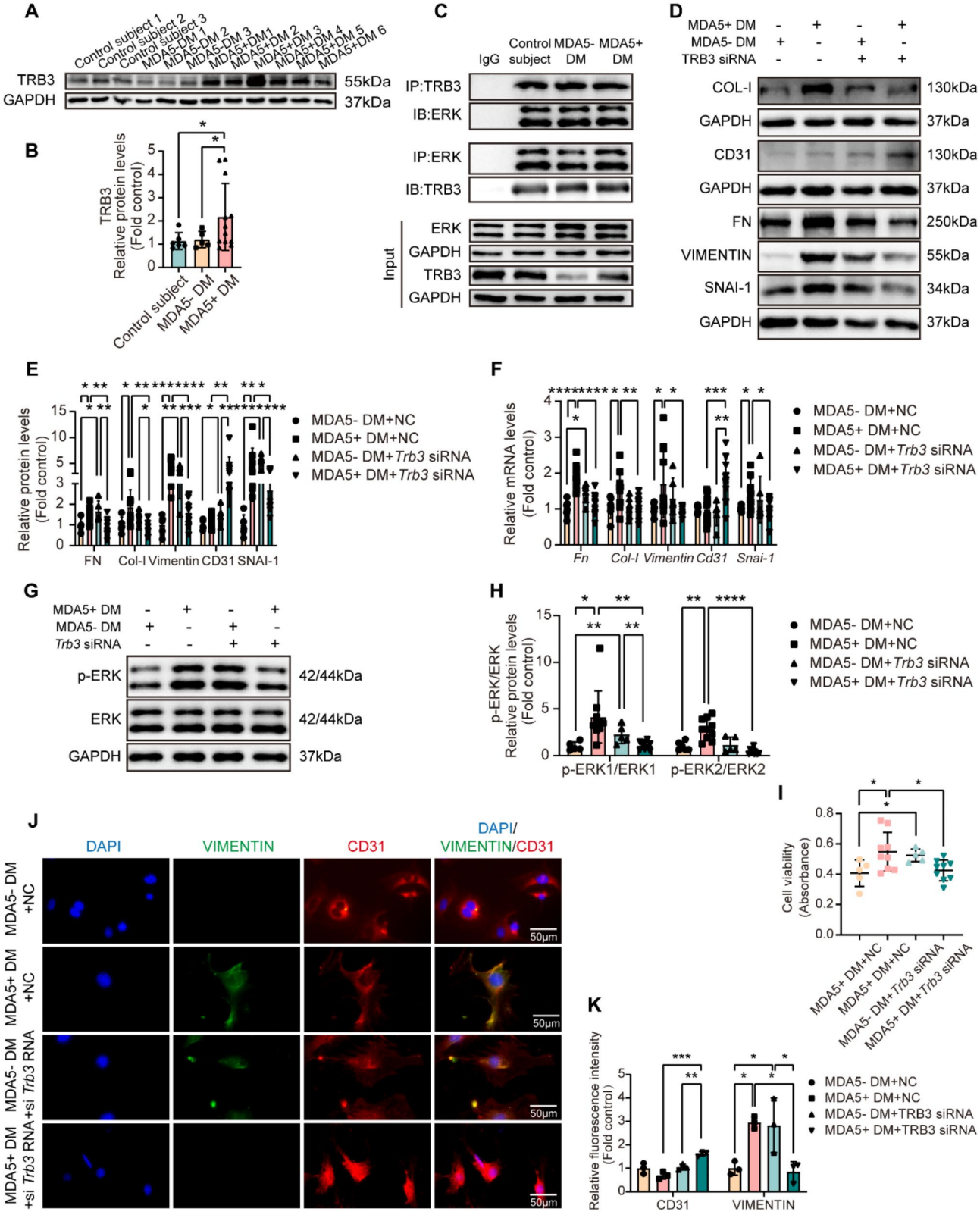

Fig. 3 (See legend on next page.)

(See figure on previous page.)

Fig. 3 TRB3 siRNA attenuated EndMT in MVECs induced by MDA5 + DM serum. (**A**, **B**) Primary mouse lung MVECs were treated with serum (10%) from control subjects, MDA5- DM and MDA5 + DM patients for 48 h. The protein levels of TRB3 were detected by Western blotting. Control subjects, $n = 6$; MDA5- DM patients, $n = 5$; MDA5 + DM patients, $n = 12$. (**C**) Cells were treated with serum for 36 h. Co-immunoprecipitation (Co-IP) was performed using anti-TRB3, anti-ERK or anti-IgG antibodies. The precipitated complex was detected using anti-TRB3 or anti-ERK. (D-K) Cells were transfected with negative control (NC) or *Trb3* siRNA, and then treated with 10% MDA5- DM serum or MDA5 + DM serum. (**D**, **E**, **G**, **H**, **J**, **K**) After siRNA transfection, the cells were treated with serum for 48 h. Expressions of proteins were measured by Western blotting (**D**, **E**, **G**, **H**, $n = 6 \sim 12$). Cell viability was assayed by CCK8 (I, $n = 5 \sim 9$). Immunofluorescence was performed to show expression and localization of protein vimentin and CD31 (**J** and **K**). (**F**) After siRNA transfection, the cells were treated with serum for 21 h. The mRNA levels were detected by qRT-PCR. $n = 6 \sim 12$. *P* values were calculated using One-way ANOVA followed by Bonferroni's test. $^{*}P < 0.05$, $^{**}P < 0.01$, $^{***}P < 0.001$, $^{****}P < 0.0001$

play a protective role in MDA5- DM serum treated-MVECs, and then backed down to normal soon. But in MDA5 + DM serum treated cells, consistent high level TRB3 induced EndMT. Consistent high level TRB3 indicated persistent ER stress/UPR existence. Thus, it needed to investigate the dynamics of ER stress/UPR.

Persistent ER stress/UPR was responsible for consistent elevated-TRB3

The UPR responds to ER stress rapidly which plays a role to release ER stress. PERK phosphorylation which indicates activation of PERK signaling is a sign of UPR. Thus, to monitor the dynamic of ER stress/UPR, PERK phosphorylation was detected in MVECs, and two time points 24 h and 48 h were set. At 24 h, TRB3 and p-PERK increased in both MDA5- DM and MDA5 + DM serum treated cells compared with control subject (Fig. 4A-D). Notably, TRB3 and p-PERK level was significantly lower in the cells treated with MDA5 + DM serum than that in MDA5- DM serum (Fig. 4A-D). At 48 h, in the MDA5- DM serum-treated cells, level of PERK phosphorylation and TRB3 recovered and was similar to the control (Figs. 3A and B and 4E and F). However, level of PERK phosphorylation and TRB3 maintained high level in MDA5 + DM serum treated cells (Figs. 3A and B and 4E and F). To furthermore confirm evidence of UPR, the other two pathways IRE1α and ATF6 signaling of UPR were detected. As shown in Fig. S10, protein changes of IRE1α and ATF6 signaling also indicated that UPR existed both in MDA5- DM and MDA5 + DM serum treated cells at 24 h, only in MDA5 + DM serum treated cells at 48 h. Moreover, ER membrane protein calnexin immunofluorescence staining was performed at 48 h, the result indicated that persistent ER stress exactly existed in MDA5 + DM serum treated cells (Fig. 4G). Furthermore, immunofluorescence staining revealed that collagen-I co-localized with PERK, indicating that EndMT accompanied with persistent ER stress/UPR in MDA5 + DM serum-treated cells at 48 h (Fig. 4H and Fig. S9).

These data suggested that MDA5- DM serum induced ER stress in MVECs and subsequently UPR relieved ER stress completely, but the MDA5 + DM serum induced insufficient UPR which resulted in persistent ER stress which was responsible for consistent elevated-TRB3.

MDA5 protein binding with PERK resulted in persistent ER stress/UPR

The mechanism of persistent ER stress/UPR in MDA5 + DM needed to further investigate. Above results indicated persistent ER stress/UPR in MDA5 + DM resulted from incomplete PERK phosphorylation in MDA5 + DM compared to MDA5- DM, then proteins which interacted with PERK were examined. As shown in Fig. 5A, proteins binding to PERK were found by immunoprecipitation and then detected using mass spectrometry, the heatmap presented top 25 proteins (expression quantity) which bound with PERK. Considering PERK phosphorylation happens in cytoplasm, and molecular function as well as biological process of protein modification, two proteins IFIH-1 and YWHAE were selected as candidate to further investigate in phosphorylating PERK (Fig. S11). YWHAE is usually recognized a phosphoserine or phosphothreonine motif which is located in the STKc domain of PERK. This domain is responsible for eIF2α phosphorylation not PERK-autophosphorylation. So, following study focused on IFIH-1. Very interestingly, IFIH-1, also named MDA5 is the specific antigen in MDA5 + DM patients.

Then, MDA5 protein in MVECs was studied. As shown in Fig. 5B and D, MDA5 proteins increased in MDA5 + DM serum-treated cells. Moreover, fluorescence co-localization, co-immunoprecipitation, and molecular docking revealed that PERK exactly interacted with MDA5 (Fig. 5E-J). MDA5 contains two caspase-recruitment domains (CARDs) at the N-terminus to activate mitochondrial antiviral signalling protein (MAVS), the central DExD/H-box helicase domain responsible for RNA-dependent ATP hydrolysis, and the C-terminal domain which selects long dsRNA with 5'ppp and blunt end and binds them. PERK contains the luminal domain sensing perturbations in protein folding, the transmembrane region, the protein kinase catalytic (PKc) domain for autophosphorylation, and the Ser/Thr protein kinase catalytic (STKc) domain to phosphorylate eIF2α in the cytoplasmic region. Based on the protein structural domains, truncated proteins of MDA5 and PERK were designed respectively to find the specific domains. In contrast to MAVS, the CTD of MDA5 was found to interact with the PKc domain of PERK (Fig. 5K and L). Seven point-mutant plasmids were designed based on

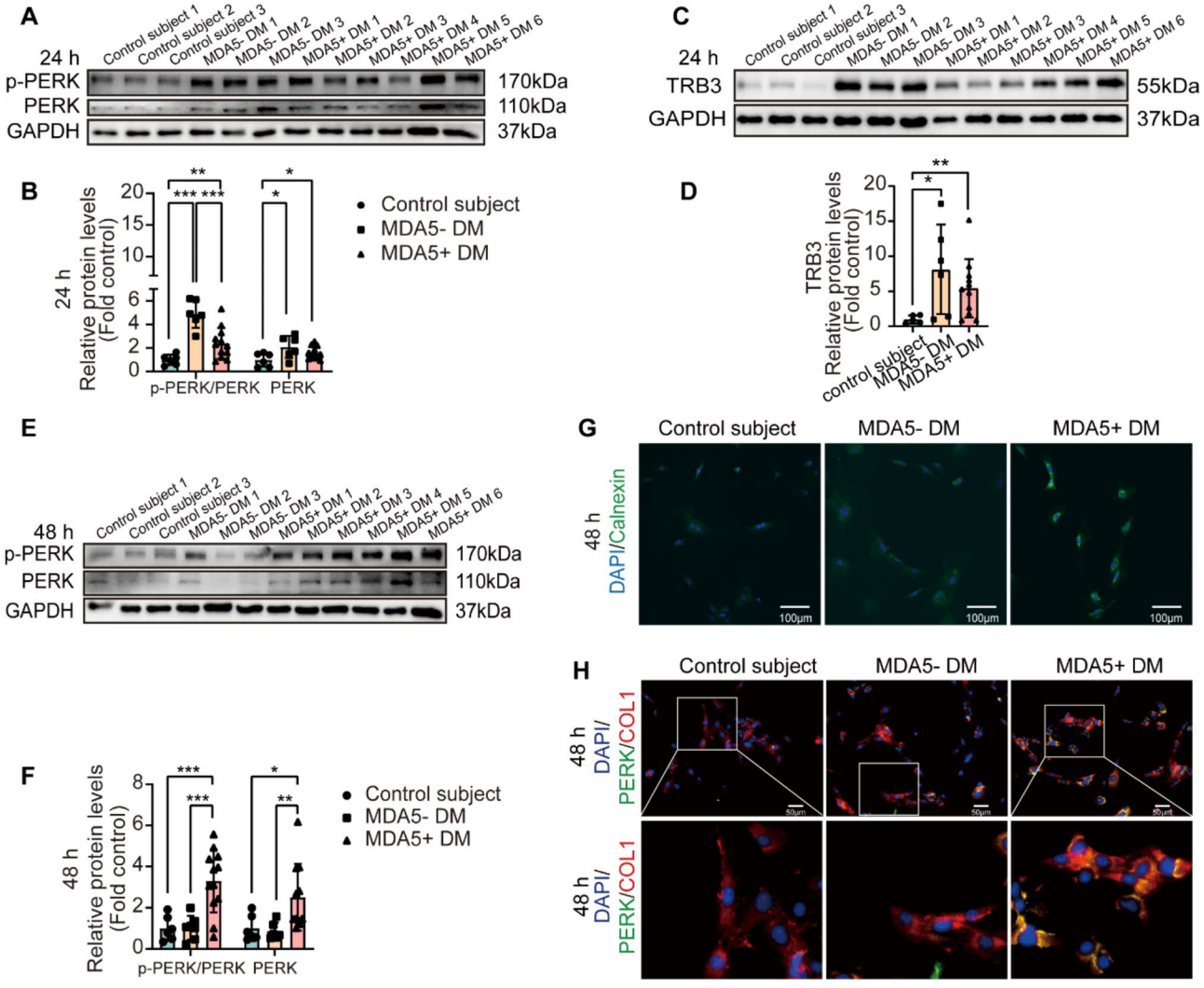

Fig. 4 MDA5 + DM serum induced persistent phosphorylation of PERK in MVECs. Primary mouse lung MVECs were treated with serum (10%) from control subjects, MDA5- DM and MDA5 + DM patients for 24 h (**A**-**D**), or 48 h (**E**-**G**). Expressions of protein were measured by Western blotting (**A**-**F**). Immunofluorescence staining was performed to show ER stress (**G**). Immunofluorescence staining was performed to reveal protein localisation of PERK and collagen I (Col-I) (**H**). Control subject, $n = 6$; MDA5- DM, $n = 6$; MDA5 + DM, $n = 12$. *P* values were calculated using One-way ANOVA followed by Bonferroni's test. $^{*}P < 0.05$, $^{**}P < 0.01$, $^{***}P < 0.001$

protein interaction sites predicted by Z-DOCK combined with single nucleotide variants provided in ClinVar. The N628S and R633Q of PERK and the G917E, E937G, E1017G and D1023A of MDA5 could affect PERK and MDA5 interaction (Fig. 5M and N).

MDA5 SiRNA prevented MDA5 + DM serum induced-EndMT

Three siRNAs for MDA5 were designed and tested their efficiency (Fig. S12A-C). siRNA1 was used as the IFIH-1 (MDA5) siRNA. This siRNA was confirmed to prevent MDA5 protein expression which was induced by MDA5 + DM serum (Fig. S12D and E). As shown in Fig. 6A, serum of MDA5 + DM patient activated ER stress at 48 h, which was inhibited by IFIH-1 siRNA. Moreover, serum of MDA5 + DM patient increased PERK phosphorylation, as well as induced EndMT in MVECs compared with MDA5- DM serum, but these were prevented by IFIH-1 siRNA (Fig. 6B-H). These data suggested that siRNA of MDA5 prevented MDA5 + DM serum induced-EndMT.

T cell from MDA5 + DM showed high expression of IFN-β, IFN-β promoted MDA5 protein expression

Then, the reason why MDA5 protein expressed in MDA5 + DM patients was explored. MDA5 protein is mainly induced by interferon (IFN). To find which IFN plays the key role in inducing MDA5 protein expression, firstly RNAs were extracted from peripheral blood mononuclear cells in control subjects and DM patients. IFN-α and IFN-β are the main members of type I IFN,

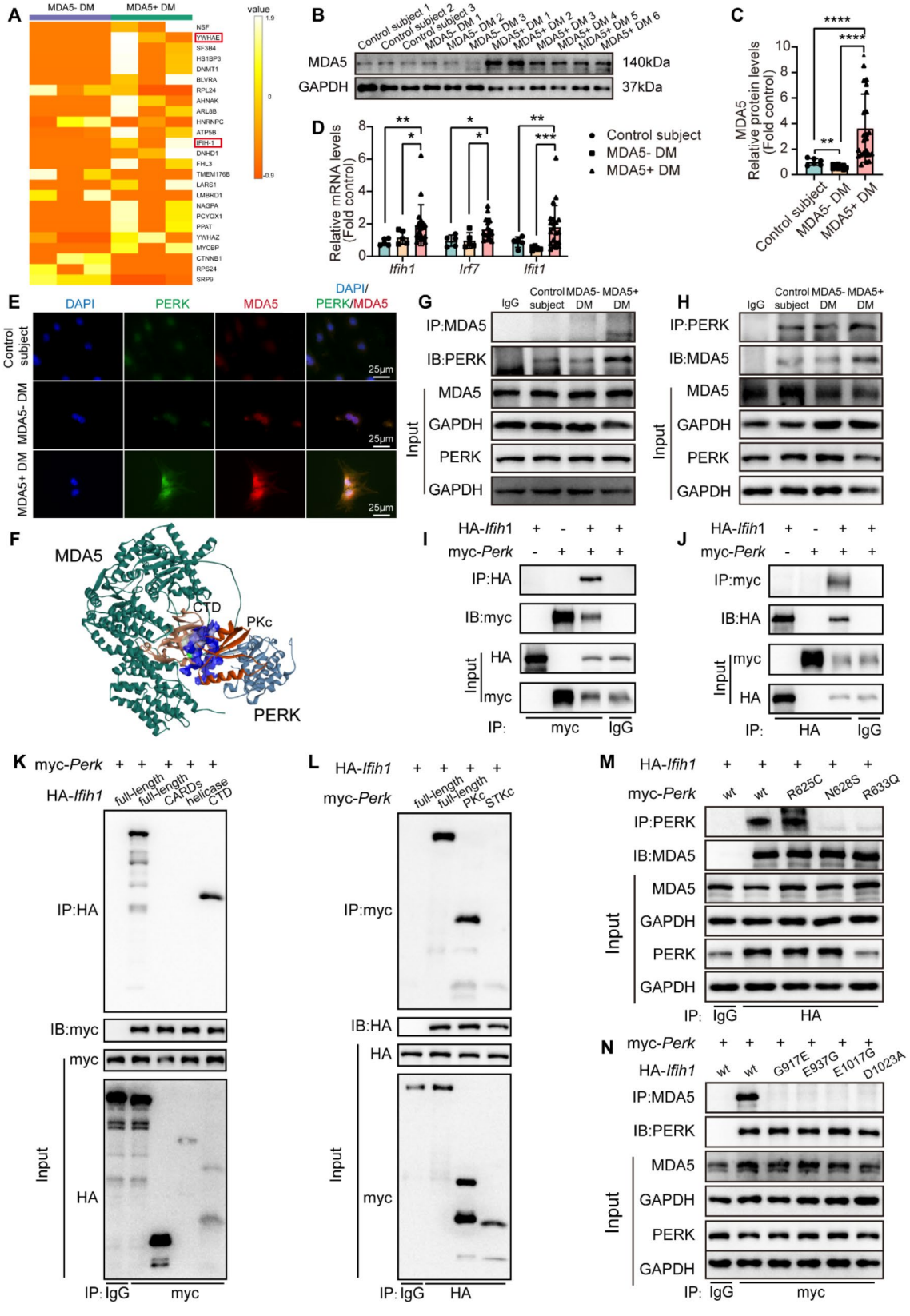

Fig. 5 (See legend on next page.)

(See figure on previous page.)

Fig. 5 Protein MDA5 increased in MDA5 + DM serum-treated MVECs and bound to PERK. (A-H) Primary mouse lung MVECs were treated with serum (10%) from control subjects, MDA5- DM and MDA5 + DM patients. (**A**-**C**) Cells were treated for 24 h, immunoprecipitation (IP) was performed using anti-PERK or anti-IgG antibodies, and interacting proteins with PERK in the precipitated complexes were analysized and showed in heatmap (**A**). Expressions of protein MDA5 were measured by Western blotting (**B**, **C**). Control subjects, $n = 6$; MDA5- DM patients, $n = 6$; MDA5 + DM patients, $n = 24$. (**D**) Cells were treated for 15 h. mRNA levels of *Ifih-1*, *Irf7* and *Ifit-1* were detected by qRT-PCR. Control subject, $n = 5$; MDA5- DM, $n = 5$; MDA5 + DM, $n = 20$). (**E**, **G**, **H**) Cells were treated for 24 h. Immunofluorescence staining was performed to reveal PERK and MDA5 (**E**). Co-IP was done using anti-MDA5, anti-PERK or anti-IgG antibodies. The precipitated complex was detected using anti-MDA5 or anti-PERK (**G**, **H**). (**F**) The schematic interaction between MDA5 and PERK was predicted by Z-dock. Green, MDA5; Claybank, the CTD of MDA5; Bice, PERK; Red, the PKc domain of PERK; Blue, proteins interaction surface. (**I**-**N**) HEK293T was transfected with HA-MDA5 plasmids, myc-PERK plasmids, truncated plasmids and point mutant plasmids for 48 h. Co-IP was performed using anti-HA, anti-myc or anti-IgG antibodies. The precipitated complex was detected using anti-HA or anti-myc. *P* values were calculated using One-way ANOVA followed by Bonferroni's test. $^{*}P < 0.05$, $^{**}P < 0.01$, $^{***}P < 0.001$, $^{****}P < 0.0001$

and IFN-γ is the main member of type II IFN. Then, IFN-α, IFN-β and IFN-γ mRNA levels were detected in peripheral blood mononuclear cells. As shown in Fig. 7A and B, IFN-α and IFN-β mRNA increased in cells from MDA5 + DM patients compared with control subjects and MDA5- DM patients. There was no difference of IFN-γ mRNA in cells from control subjects, MDA5- DM or MDA5 + DM patients. Next, peripheral blood mononuclear cells from healthy donors were treated with IFN-α and IFN-β (Fig. S13A and B), differentially expressed genes were detected, IFN-α- and IFN-β-regulated top 10 genes were found (Fig. S13C and D). Then, top 3 IFN-α- and IFN-β-regulated genes were detected in RNAs extracted from peripheral blood mononuclear cells in control subjects and DM patients. As shown in Fig. SE and F, top 3 IFN-α-regulated genes did not increase, but 2 of 3 top genes which were regulated by IFN-β increased. These results indicated IFN-β rather than IFN-α should contribute to MDA5 expression. Then, using anti-IFN-β antibody to inhibit IFN-β in the serum. As shown in Fig. 7C, MDA5 + DM serum induced expressions of MDA5 protein in MVECs, but these was prevented by anti-IFN-β antibody.

To further understand the role of IFN-β in MDA5 expression and EndMT in MVECs, IFN-β was used to directly treat primary mouse lung MVECs without MDA5 + DM serum. As shown in Fig. S14A and B, IFN-β induced MDA5 protein expression in MVECs. However, IFN-β did not induce UPR or EndMT (Fig. S14C-F). These data indicated that IFN-beta/MDA5 mediated EndMT, which must base on ER stress induced by MDA5 + DM serum.

To further understand which type cells contributed to production of IFN-β, mean fluorescence intensity (MFI) of IFN-β was detected in peripheral blood mononuclear cells in control subjects and DM patients. Followed the flow cytometry gating strategy of human peripheral blood mononuclear cells (Fig. S15), T cells, B cells, NK cells, DC and monocytes were identified. As shown in Fig. 7D and E, it was found that IFN-β increased in T cells rather than B cells, NK cells, DC or monocytes.

These data suggested that T cell-derived-IFN-β promoted MDA5 protein expression in lung MVECs in MDA5 + DM.

Discussion

In this study, firstly based on clinical data, analysis revealed that vascular damage and ILD was correlated with anti-MDA5 antibody in DM patients. Then, serum from patients was used to treat vascular endothelial cells in vitro. It was found that serum from MDA5 + DM patients induced EndMT in mouse lung MVECs, and the EndMT in MVECs was mediated by TRB3/ERK/Snai-1 pathway. Next, up-stream of TRB3 was explored. Persistent ER stress/UPR was found leading to consistent elevated-TRB3 in MVECs. MDA5 protein binding with PERK was involved in persistent ER stress/UPR. At last, T cell-derived IFN-β was confirmed to induce MDA5 expression in MDA5 + DM patients. Taken together, MDA5 protein mediating persistent ER stress/UPR contributed to EndMT of lung microvascular endothelial cells in MDA5 + DM patients, which should be involved in MDA5 + DM-related ILD.

ER stress is a disruption of ER homeostasis, and abnormal perturbations including intrinsic and extrinsic perturbations can cause ER stress. Intrinsic perturbations caused by cell autonomous mechanisms, such as uncontrolled protein synthesis required for cancer cell growth, accumulation of mutant proteins and abnormal protein transport vesicles [24]. Extrinsic perturbations were mainly from abnormality of cellular microenvironment. In this study, serum from DM patient treatment with MVECs caused ER stress, it suggested that microenvironmental abnormality was responsible for ER stress. We did not investigate detailed causes of ER stress here. Severe immunosuppression, immune dysfunction and coagulation activation was observed in MDA5 + DM, these microenvironments should be causes of ER stress [25]. The disruption to homeostasis is more severe in MDA5 + DM patients than in MDA5- DM patients. ER stress is also seen in normal physiological situations, such as high metabolic demands or large amounts of protein synthesis in process of embryonic development and growth differentiation [26–28]. Physiological ER stress/

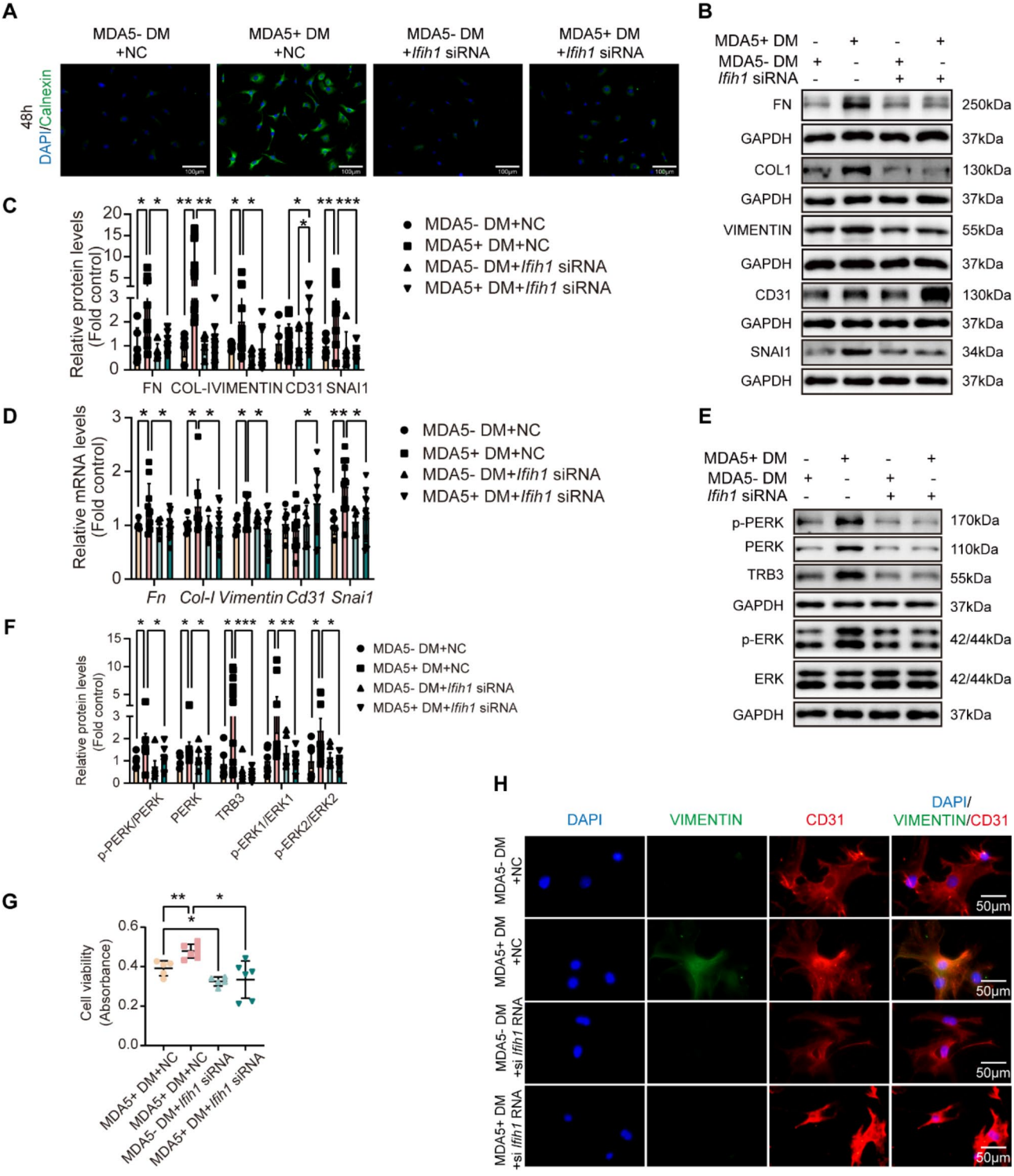

Fig. 6 MDA5 siRNA attenuated MDA5 + DM serum-induced EndMT in MVECs. Primary mouse lung MVECs were transfected with negative control (NC) or MDA5 siRNA and then treated with 10% MDA5- DM serum or MDA5 + DM serum. Cells were treated with serum for 48 h. Immunofluorescence staining was performed to show ER stress (**A**). Protein expressions were detected by Western blotting (**B**, **C**, **E**, **F**). Cell viability was assayed by CCK8 (**G**). $n = 5 \sim 6$. Immunofluorescence staining was performed to show vimentin and CD31 (**H**). (**D**) Cells were treated with serum for 21 h. mRNA levels were detected by qRT-PCR. $n = 6 \sim 12$. *P* values were calculated using Unpaired t test, Welch's t test or One-way ANOVA followed by Bonferroni's test. $^{*}P < 0.05$, $^{**}P < 0.01$, $^{***}P < 0.001$, $^{****}P < 0.0001$

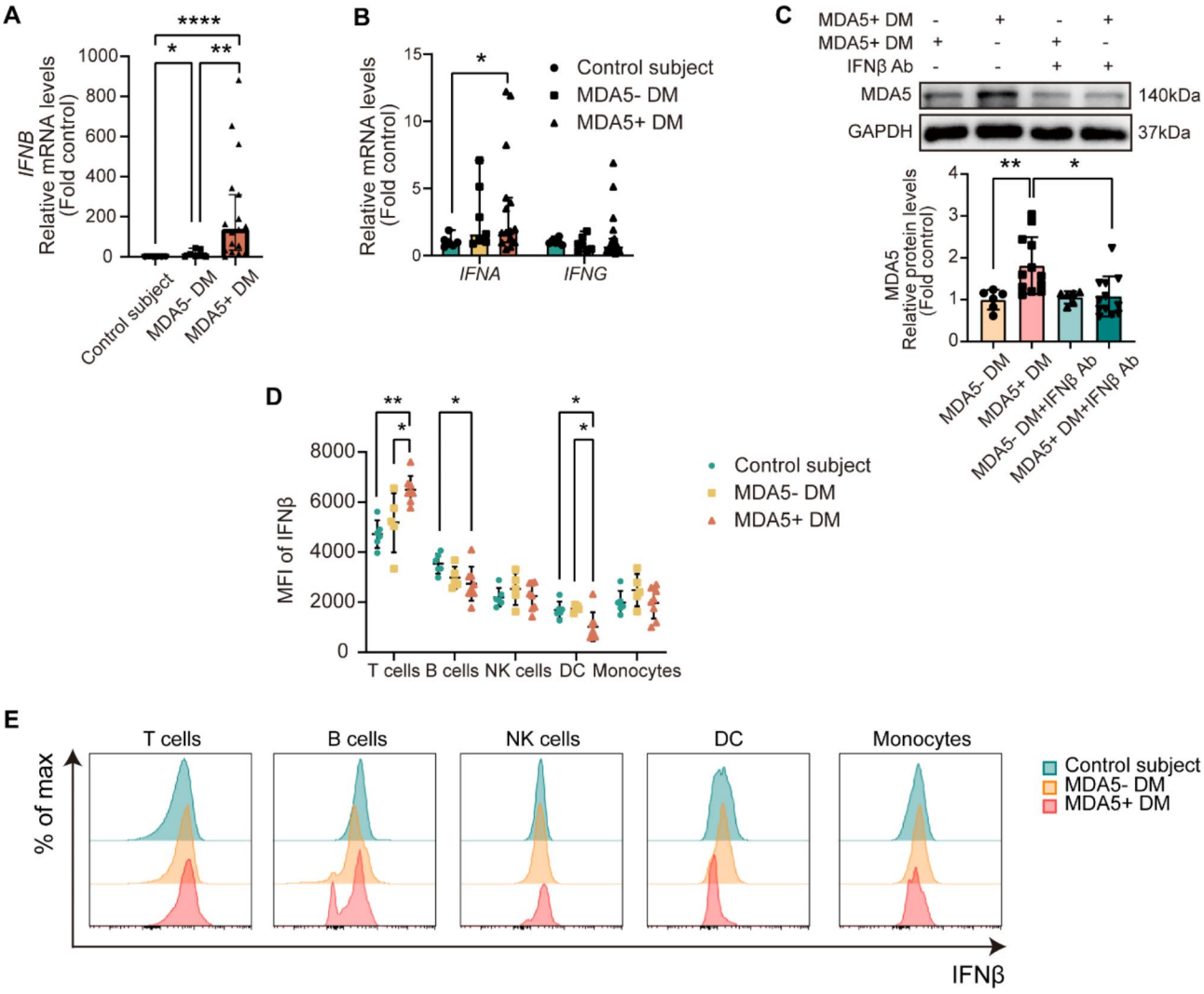

Fig. 7 T cell-derived IFN-β induced MDA5 expression. (**A**, **B**) RNA was extracted from peripheral blood mononuclear cells in control subjects and DM patients. mRNA levels of IFN-β, IFN-α and IFN-γ were determined by qRT-PCR. Control subject, $n=6$; MDA5- DM, $n=7$; MDA5 + DM, $n=17$. (**C**) Primary mouse lung MVECs were pre-incubated with or without 0.5 μg/ml IFN-β neutralizing antibodies (IFN-β Ab) and then treated with 10% MDA5- DM serum or MDA5 + DM serum. Expression of MDA5 was measured by Western blotting. MDA5- DM, $n=6$; MDA5 + DM, $n=12$; MDA5- DM + IFN-β Ab, $n=6$; MDA5 + DM + IFN-β Ab, $n=12$. (**D**) Mean fluorescence intensity (MFI) of IFN-β in main cell types of peripheral blood mononuclear cells. Control subject, $n=6$; MDA5- DM, $n=5$; MDA5 + DM, $n=8$. (**E**) Representative fluorescence intensity histogram of IFN-β in main cell types of peripheral blood mononuclear cells. *P* values were calculated using One-way ANOVA followed by Bonferroni's test. $^{*}P<0.05$, $^{**}P<0.01$, $^{***}P<0.001$, $^{****}P<0.0001$

UPR is usually transient and temporary. In the current study, temporary ER stress/UPR existed in MDA5- DM serum-treated cells, and persistent ER stress/UPR existed in MDA5 + DM serum-treated cells which mediated vascular endothelial cell EndMT.

EndMT is considered as an over-repair process after damage in endothelial cell, which contributed to ILD and lung fibrosis [29]. Results from studies including the current study revealed that the incidence of ILD was much high in MDA5 + DM patients compared with MDA5- DM patients. Thus, in this study, serum from DM patients were used to treat MVECs and their EndMT was investigated. EndMT was exactly activated in MDA5 + DM serum-treated cells. Subsequently, EndMT in MVECs was confirmed mediating by TRB3/ERK/Snai-1 pathway. Reports displayed that TRB3 was involved in persistent ER stress/UPR [30]. However, TRB3 alteration was little known in temporary persistent ER stress/UPR. Based on different findings of dynamic changes of ER stress/UPR in MDA5 + DM and MDA5- DM treated cells, we thought TRB3 increased and recovered in temporary ER stress/UPR. On the contrary, relatively light and consistent increases of TRB3 existed in insufficient UPR and persistent ER stress/UPR. TRB3, acting as a bridge between ER stress/UPR and other pathways, is involved in the fibrosis process of a variety of organs. In pulmonary fibrosis,

TRB3 promotes fibroblast activation by interacting with P62, or activates the SMAD pathway or WNT pathway to promote epithelial mesenchymal transformation (EMT) in alveolar epithelial cells [31–33]. Our results showed that TRB3 activated ERK pathway in MVECs to promote EndMT which was involved in pulmonary fibrosis. These researches including our current study indicated that TRB3 could activate different signaling pathways in different kinds of cells, then mediated EndMT or EMT.

Moreover, we traced molecular signaling pathways, MDA5 protein was confirmed as the key regulator in insufficient UPR as well as persistent ER stress/UPR. In normal condition, MDA5 hardly expressed in human body. The exactly mechanism of MDA5 expression was still unclear, it is generally thought that MDA5 expression resulted from increases of IFN when body recognition of aberrant double-stranded nucleotides [34, 35]. Our results revealed that serum IFN-β caused elevated MDA5 expression in endothelial cells. Previous studies showed that IFN-β had a greater impact on DM than IFN-α or IFN-ω did [36, 37]. These indicated that IFN-β was a potential marker as an early specific indicator of disease activity. However, this study also indicated that EndMT induced by serum from MDA5 + DM but not only due to high IFN-β. A number of genetic variants have been found to result in accumulation of abnormal double-stranded DNA or RNA, which in turn activated MDA5 and led to development of IFN associated diseases. Genes with single nucleotide variants (SNV) related to DM or DM-related ILD included WDFY4, NFRκB, ZFP57, ATF7IP2, ZNF697, LILRB2, AGER, HLA-DQB1, HLA-DQA1, HLA-DRB1, and ANKRD55 [38–41].

Previous concerned researches focused on interaction of MDA5 with mitochondrial-outer membrane protein mitochondrial antiviral signalling protein (MAVS) [42]. It got much more attention about MDA5 interaction with endoplasmic reticulum membrane protein PERK [43]. Based on genetic information provided by ClinVar, N628S (1883 A > G), R633Q (1873 C > T) in PERK, and G917E (2750G > A), E937G (2810 A > G), E1017G (3050 A > G), D1023A (3067G > T) in MDA5 played their role in interactions between PERK and MDA5 protein. In the current study, MDA5 binding with PERK and regulating ER stress/UPR was elucidated. Further studies about MDA5 interacting with other organelle membrane proteins are needed.

Drugs used in treatment of DM include glucocorticoids, calcium-modulated phosphatase inhibitors, antimalarials, Janus kinase inhibitors, biologic monoclonal antibodies, etc. The rational use of those drugs should take into account the types of DM [44]. As for MDA5 + DM, combination immunosuppressive therapy was commonly used. It is worth noting that anti-fibrotic therapy improved long-term quality of life in MDA5 + DM patients [45, 46]. Our findings support the idea of anti-fibrotic therapy in MDA5 + DM patients, and suggested that anti-fibrotic therapy was started at early stage of the disease.

Moreover, in our experiments, *Trb3* siRNA increased TRB3 protein in the cells co-cultured with serum from MDA5- DM patients (Fig. S7D, Fig. S8C). We also measured the mRNA level, TRB3 siRNA exactly decreased TRB3 mRNA in the cells (Fig. S7F). These results indicated that TRB3 siRNA inhibited mRNA but failed to decrease protein of TRB3 in the cells co-cultured with serum from MDA5- DM patients. We speculated that the reason for this phenomenon may be the existence of temporary ER stress/UPR in the cells treated by serum from MDA5- DM patients. In temporary ER stress/UPR, a high level of TRB3 was necessary to feedback suppress the ER stress, when TRB3 was inhibited by TRB3 siRNA, the ER stress did not feedback stop and turned into persistence. Thus, more TRB3 protein produced.

Limitations of this study include: (1) The sample size was not very large, although subjects all met the criteria. (2) Because of the accessibility of materials, we only did EndMT using human lung microvascular endothelial cells, and did other experiments using mouse lung microvascular endothelial cells instead of human cells. (3) In our experiments, *Trb3* siRNA increased TRB3 protein in the cells co-cultured with serum from MDA5-DM patients. We did not know the exact mechanism. (4) The serum was derived from patients at different stage of DM, which may be one of the reasons for variation in the groups. (5) As a retrospective cohort study in clinical analysis, some laboratory indicators missed in a small number of patients.

Methods

Patients and clinical data

A total of 127 patients, including 64 patients with anti-MDA5 + DM and 63 patients with other myositis-specific antibodies (MSAs) positive, were recruited from January 2018 and May 2024 at the Department of Rheumatology or Department of Respiratory and Critical Care Medicine, Union Hospital, Wuhan, China. The study protocol was approved by the Ethics Committee of Union Hospital (ID: S1220), Wuhan, China. This part of the study was conducted according to the Declaration of Helsinki. All DM patients fulfilled the EULAR/ACR classification criteria (IIM calculator - English version) for idiopathic inflammatory myopathies (IIM) 2017 (min IIM Probability ≥ 90%) and screened for myositis-specific autoantibodies (MSAs) and myositis-associated autoantibodies (MAAs), referencing previous studies [47]. The data were retrospectively obtained, including demographic information, clinical features, laboratory indices, scoring of HRCT findings. Assessment of skin involvement was

based on the Disease Activity Score (DAS) for DM. The DAS score was performed by analysis of the distribution and severity of skin involved, which included Gottron sign/papules and mucocutaneous vasculature. The severity of the involved skin was rated on a 5-point scale, ranging from absent to severe. The distribution of the involved skin was rated on a 4-point scale, ranging from none to generalized. Ulceration belonged to severe skin involvement. The DAS skin score ranged 0–9. More details can be referenced to the literatures [48, 49].

Serum and peripheral blood mononuclear cells isolation

Whole blood was collected in the ethylenediaminetetraacetic acid tube to isolate peripheral blood mononuclear cells, additive-free tube to obtain serum. Samples were collected on the first day of admission in the hospital and stored at 4℃ before isolation. The peripheral blood mononuclear cells were isolated using the Human Whole Blood Mononuclear Cell Isolation Solution (TBD, LDS1075), and erythrocytes were lysed with red blood cell lysis buffer (biosharp, BL503B). All operations were following the manufacturer's instructions. Additive-free tubes were at room temperature 30 min after blood collection. Then, centrifuge at 3, 000 rpm for 15 min and aliquots of serum were frozen at -80℃.

Myositis specific antibody (MSA) detection

Antibodies were detected by using commercial dot immunoassays kits. Grey-scale values were defined accordingly: 0 to 5 units/L as negative, 5–10 units/L as probable positive, 11 to 40 units/L as weak positive, 41 to 70 units/L as positive, and >70 units/L as strong positive. The antibody in the gray area was considered to be absent, while the weak positive sample was judged by repeated test.

Isolating primary mouse lung microvascular endothelial cells (MVECs)

Mice were euthanized with pentobarbital sodium (0.2 mg/g) and sterilized with 75% alcohol. Cut the thorax to expose the lungs and heart. Operator held smooth forceps in both hands, one hand picked up apex of heart, and the other hand tore out left auricle. Perfusion was performed from right ventricle with 10 ml PBS. Aseptically excised individual lung lobes and washed them in cold PBS. Cut off and mince finely the lung edges and surface tissue. These obtained lung tissues were transfered into warm collagenase solution (2 mg/mL collagenase (Sigma, St. Louis, MO, USA) and DNase I 2 μg/mL (Sigma)) for enzymatic digestion, then were incubated for 30 min at 37℃. Using a 5 ml needle to triturate clumps into a single-cell suspension. The suspension was passed through a 40 μm cell strainer and washed with a complete culture medium, then centrifuged at 400 g for 5 min and removed supernatant.

Mix CD31 microbeads (Miltenyi, 130097418) with cell pellet were incubated on a vertical rotator for 15 min. Cells were washed by adding 3 ml rinsing buffer (Miltenyi, 130091222) and centrifuged at 400 g for 5 min. Prepared the LS columns (Miltenyi, 130042401) by rinsing with rinsing buffer. Resuspend the cells with 3 ml rinsing buffer, then applied the cell suspension onto the column. The column was washed with 3 ml buffer three times. Removed the column from the MidiMACS™ Separator (Miltenyi, 130042302), and pipetted 6 ml buffer onto the column. The plunger was firmly pushed into the column, then the magnetically labeled cells were flushed out. Centrifuged at 400 g for 5 min. Resuspend CD31-positive cells were cultured in Endothelial Cell Medium with 15% fetal calf serum (FBS), endothelial cell growth supplement and antibiotic solution (ECM, ScienCell, #1001). The cells at passage second to 5th were used in experiments except for flow cytometry.

Cell culture and transfection

Primary mouse lung MVECs were cultured in complete ECM medium, and passaged at ratio 1: 2. Human lung MVECs, HULEC-5a cells were obtained from American Type Culture Collection (ATCC, CRL3244) and cultured in MCDB131 (Gibco, 10372019) with 10% FBS, 10 ng/mL epidermal growth factor (EGF), 1 μg/mL hydrocortisone and 10 mM glutamine. HEK293T (ATCC, CRL-1573.3) cells were cultured in high-glucose DMEM medium (Gibco, C11995500BI) supplemented with 10% fetal bovine serum (Gibco, 10100147). The cells were passaged at ratio 1: 3. All culture media contained penicillin (100 U/ml) and streptomycin (100 μg/ml). Cells were maintained at 37 °C in a humidified atmosphere containing 5% CO_2.

For plasmids transfection, Neofect™ solution (Neofect Biotechnologies, Shanghai, China, TF201201) was mixed with plasmids according to the instruction manual. Waiting for 15 min, HEK293T were transfected with the Neofect™-plasmids complexes. Transfected cells were harvested 48 h after treatment. The pcDNA3.1-EIF2AK3-Myc-Neo plasmid and pcDNA3.1-IFIH1-HA-Neo plasmid were purchased from Miaoling (Wuhan, China). The pcDNA3.1-IFIH1 1-207 aa-HA-Neo, pcDNA3.1-IFIH1 298–899 aa-HA-Neo, pcDNA3.1-IFIH1 900–1025 aa-HA-EGFP-Neo, pcDNA3.1-EIF2AK3 586–675 aa-Myc-EGFP-Neo, pcDNA3.1-EIF2AK3 873–1075 aa-Myc-Neo plasmids were purchased from Fenghbio (Hunan, China). All vectors were confirmed by DNA sequencing.

For siRNA transfection, specific gene siRNA (Tsingke, Beijing, China) and Lipofectamine RNAiMAX reagents (Invitrogen, Carlsbad, USA, 2297560) were premixed in opti-MEM™ (Gibco,

31985070) for 20 min and added to serum-free and antibiotic-free medium. The sequences for siRNAs targeting specific genes were as follows: *Trb3* siRNA1 sense 5′-CCAAGUGUCCAGUCCUAAA-3′, anti-sense 5′-UUUAGGACUGGACACUUGG-3′; siRNA2 sense 5′-GCACAGAGUACACCUGCAA-3′, anti-sense 5′-UUGCAGGUGUACU CUGUGC-3′; siRNA3 sense 5′-GUCGCUUUGUCUUCAGCAA-3′, anti-sense 5′-UU GCUGAAGACAAAGCGAC-3′. *Ifih1* siRNA1 sense 5′-CGAGAGAAGAUGAUGUAUAA A-3′, anti-sense 5′-UAUACAUCAUCUUCUCUCGGA-3′; siRNA2 sense 5′-GGUAAUGUUAGCAGAACAACU-3′, anti-sense 5′-UUGUUCUGCUAACAUUACCUU-3′; siRNA3 sense 5′-CAGAAGUUGUCAAAUCUUACG-3′, anti-sense 5′-UAAGAUUUGACAACU UCUGG A-3′. Negative control siRNA sense 5′-UUCUCCGAACGUGUCACGUTT-3′, anti-sense 5′-ACGUGACACGUUCGGAGAATT-3′. *Trb3* siRNA1, siRNA2, siRNA3 and *Ifih1* siRNA1, siRNA2, siRNA3 were used in the experiments of knockdown efficiency tests, and only *Trb3* siRNA3 and *Ifih1* siRNA1 were selected to do follow-up experiments.

Flow cytometry

Cell suspensions were incubated with a Fixable Fc block at room temperature for 15 min. Then, cells were stained with FVS (BioLegend, Zombie NIR™ Fixable Viability Kit) at room temperature for 20 min and washed with 1% FBS in PBS. The cells were mixed with the fluorophore-conjugated antibodies and incubated at 4℃ for 30 min in the dark. After twice washes, cells were resuspended in PBS. Flow cytometry was performed on 5 lasers full spectrum flow cytometer (Sony, ID7000) and data were analyzed with FlowJo software (Tree Star).

The following anti-human antibodies were obtained from BD Biosciences, BioLegend or eBioscience™: FITC anti-IFNβ (A1), BB515 anti-CD3 (HIT3a), BUV395 anti-CD4 (RPA-T4), BV421 anti-CD8 (RPA-T8), BV510 anti-CD19 (SJ25C1), AF700 anti-CD14 (M5E2), PE-Cy7 anti-CD56 (B159), AF647 anti-CD16 (3G8), PerCP-Cy5.5 anti-HLA DR (G46-6), BV605 anti-CD11c (3.9), PE anti-CD123 (S18016C). Anti-mouse antibodies were also obtained from Biolegend: APC anti-mouse CD31 (MEC13.3).

Western blotting

Mouse lung MVECs were harvested and lysed in ice-cold RIPA lysis buffer (1% NP-40, 1% SDS, 5% Sodium deoxycholate) containing a phosphatase inhibitor (Roche, Basel, Switzerland, 539,142) and protease inhibitor cocktail (Calbiochem, San Diego, CA, 539,131). The protein concentration was measured by a BCA assay kit (Thermo, Waltham, MA, 23,225). Western blotting was performed according to a standard method. The dilution concentrations of primary antibodies were as follows: CD31 (1:750, Abclonal, A4900), FN (1:1000, Proteintech,15612-1-AP), Col-I (1:1000, Bioswamp, PAB31604), Vimentin (1:1000, Proteintech, 10366-1-AP), Snai-1 (1:1000, Abclonal, A5243), p-ERK (1:1000, CST, #4370), ERK (1:1000, CST, #4695), p-SMDA2/3 (1:1000, CST, #8828), SMAD2/3 (1:1000, CST, #8685), SMAD4 (1:1000, Abclonal, A19116), p-PI3K (1:1000, CST,17366), PI3K (1:1000, CST, 4292 S), p-p65 (1:1000, Abclonal, AP0475), p65 (1:1000, Abclonal, A22676), TRB3 (1:1000, Proteintech, 13300-1-AP), p-JNK (1:1000, Abmart, T40074), JNK (1:1000, Abmart, T40073), p-p38 (1:1000, Abmart, T40076), p38 (1:1000, Abmart, T40076), p-PERK (1:1000, Affinity, DF7576), PERK (1:750, Abclonal, A18196), MDA5 (1:1000, Proteintech, 21775-1-AP), GAPDH (1:5000, Proteintech, 60003-1-Ig), p-MEK1/MEK2 (1:750, Abclonal, AP0209), MEK1/MEK2 (1:1000, Abclonal, A18117), p-EGFR (1:750, Abclonal, AP0027), EGFR (1:1000, Abclonal, A11082), p-Ret (1:750, Abclonal, AP0600), Ret (1:1000, Abclonal, A20845), p-Jak2 (1:750, Abclonal, AP0600), Jak2 (1:1000, Abclonal, A20845), ATF6 (1:1000, Abclonal, A0202), p-IRE1α (1:800, Abclonal, AP0878), IRE1α (1:1000, Abclonal, A21021).

Primary antibodies were incubated at 4 °C overnight. HRP-conjugated secondary antibodies (service, Wuhan, China) were incubated at room temperature for 2 h (dilution 1:5000), and then the HRP activity-based signal detected by the ChemiScope 6000 system (Clinx, Shanghai, China). Using IpWin5 software measured band intensity.

RNA extraction and quantitative real-time polymerase chain reaction (qRT-PCR)

Total RNA was extracted from primary mouse lung MVECs or human peripheral blood mononuclear cells with Trizol (Vazyme, R401-01). mRNA was converted to cDNA by the Hiscript@ Q RT SuperMix (Vazyme, Nanjing, China, R223-01), and qRT-PCR was performed using the Cham Q SYBR qPCR Master Mix (Vazyme, Q311-02) and specific primers on PCR System 9700 (GeneAmp, USA). Gene expression levels were normalized to *GAPDH* or *HRPT1* and quantified with the $2^{-\Delta\Delta CT}$ relative quantification method. The information on primers was presented in Table S3.

CCK-8 assay

Primary mouse lung MVECs were seeded in 96-well plates (6×10^3 cells/well). 10 μl CCK-8 reagent (Targetmol) was added to each well. The plates were incubated at 37℃ for 2 h. The optical density (OD) value at 450 nm wavelength was measured to compare cell growth activity.

Immunofluorescence staining

Cells were plated on the slides at least 24 h before treatment. Cells were fixed with 4% paraformaldehyde (PFA) for 15 min and permeabilized with 0.5% Triton X-100 for 10 min. The slides were washed two times, and the cells were blocked by 5% Bovine serum albumin (BSA, Servicebio, G5001-100G) in PBS for 1 h, then incubated with primary antibodies at 4 °C overnight. The dilution concentrations of primary antibodies were as follows: α-SMA (1:100, Proteintech, 80008-1-RR), SFTPC (1:150, Proteintech, 10774-1-AP), CD31 (1:100, Abclonal, A4900), Calnexin (1:200, Proteintech, 66903-1-Ig), Col-I (1:100, Bioswamp, PAB31604), MDA5 (1:100, Proteintech, 21775-1-AP), PERK (1:100, Abclonal, A18196). According to different species of the primary antibodies, Cy3-or FITC-labeled rabbit or mouse secondary antibodies (dilution 1:200) were incubated for 1.5 h at room temperature in the dark. For the same species, ABflo® 594-conjugated rabbit secondary antibody and ABflo® 488-conjugated rabbit secondary antibody was used. The nuclei in cells were stained with DAPI (Servicebio, G1012) at room temperature in the dark for 8 min. The fluorescence images were observed by Zeiss-LSM780 confocal laser scanning microscope (Carl Zeiss AG, Oberkochen, German) or Leica-DMi8 inverted fluorescence microscope (Leica, German).

Co-immunoprecipitation (Co-IP) assay

Primary mouse lung MVECs or 293T were harvested and lysed in IP lysis buffer (1% NP-40, 50 mM Tris-HCl (pH = 7.4), 150 mM NaCl, 2 mM EDTA, 50 mM NaF, 10% glycerol) containing protease inhibitor cocktail at 4 °C for 2 h. Then supernatants were gathered after centrifugation. The protein concentrations were quantified as above description. The lysate was mixed with appropriate antibodies according to the instructions and incubated at 4 °C on a vertical rotator overnight. The supernatants were gathered after centrifugation at 14, 000 rpm for 15 min at 4 °C. Cell lysates containing the antibody were incubated with protein A/G magnetic beads (MCE, HY-K0202) at 4 °C on a vertical rotator for 2 h. The complexes, containing Magnetic beads, antibodies, bait protein, and target proteins, were separated from cell lysates in the magnetic stand. The complexes were washed with lysis buffer two times and further with PBS two times. The Protein A/G Magnetic Beads-Ab-Ag complexes were resuspended in lysis buffer and mixed with 2 × SDS-PAGE Loading Buffer. Protein expressions were determined by western blotting as described above to detect interrelationships of the related proteins.

Protein mass spectrometry

The samples were divided into three groups and each group contained three samples. Protein solutions were prepared by IP method with anti-PERK antibody (CST, #5683T). The protein concentration was measured by Bradford assay kit (Beyotime, P0006). The protein in the solution was digested with trypsin at ratio 1: 100. The digested protein solutions were desalinated and vacuum-dried by a frozen vacuum concentrator (Concentrator Plus 5305, Eppendorf). Peptides were separated and identified by a Q ExactiveHF mass spectrometer. The raw data was searched in a proteomics database and analyzed to find differentially expressed proteins. Parameters for classifying significantly DEGs were as follows: FC > 1.2 and $p < 0.05$, FC: the fold change of expressions. The functional annotation database of DEGs was carried out using multiple databases, including COG, GO, and Kyoto Encyclopedia of Genes and Genome (KEGG).

Protein-protein Docking

Three-dimensional structures of proteins were downloaded from RCSB PDB (https://www.rcsb.org). For PERK (4 × 7k) and MDA5 (7JL0) were large molecules, rigid molecular docking was performed by Z-dock (https://zdock.umassmed.edu/). Docking results were analyzed on the PDBePISA (https://www.ebi.ac.uk/msd-srv/prot_int/cgi-bin/piserver) and filtered according to free energy (ΔiG), ΔiG P-value and interface area (Å2). The docking result was visualized by Discovery Studio 4.5 (Biovia).

Protein kinases identification

Searched the kinases that phosphorylate ERK on the PhosphoSitePlus® (https://www.phosphosite.org/homeAction.action). Then, the kinases were constructed as protein-protein interaction (PPI) networks on The Search Tool for the Retrieval of Interacting Genes (https://cn.string-db.org/).

Statistical analysis

he clinical data were analyzed by the SPSS (version 22.0; SPSS, Inc., Chicago, IL). The experimental data were analyzed with Prism software version 8.0.2. Quantitative variables for two groups were tested by F-test and then selected unpaired t-test or Welch's t-test based on the homogeneity of variance to calculate the P-value. For at least three groups, the Brown-Forsythe test or Bartlett's test was used to verify homogeneity of variance, and the one-way ANOVA test was used to check the difference followed by Bonferroni's test. Multiple comparisons were taken to compare pairwise according to ANOVA results. The data were presented as the mean ± SD. A P-value < 0.05 was considered significant. Qualitative variables were presented as frequencies or percentages and compared via the Wilcoxon rank sum test or chi-square test. If the P-value of the chi-square test was near 0.05,

Fisher's exact test was applied. The correlation test was performed by Pearson's Correlation Tests.

Abbreviations

DM	Dermatomyositis
EndMT	Endothelial-to-mesenchymal transition
ER	Endoplasmic reticulum
IFN	Interferon
ILD	Interstitial lung disease
MDA5	Melanoma differentiation-associated gene 5 protein
MDA5 + DM	Anti-MDA5 antibody positive
MDA5- DM	And anti-MDA5 antibody negative
MVECs	Microvascular endothelial cells
PERK	Protein kinase RNA-like ER kinase
TRB3	Tribbles homolog 3
UPR	Unfolded protein response

Supplementary Information

The online version contains supplementary material available at https://doi.org/10.1186/s12964-025-02159-2.

Supplementary Material 1

Acknowledgements
All authors appreciate the Medical Sub-Center of Analytical & Testing Center at the Huazhong University of Science and Technology for technical supports.

Author contributions
H. Y. and W. L. M. conceived the study. L. Q. Z. designed the experiments. L. Q. Z., X. F., H. D. Z. and S. Y. Y. performed the experiments. L. Q. Z., X. Q. Y. and Q. N. collected clinical data. L. Q. Z. and X. Q. Y. analyzed the data. L. Q. Z., X. F., Q. N., L. J. J. and F. Y. collected clinical samples. L. Q. Z., H. Y., and W. L. M. prepared the figures and wrote the manuscript with input from all authors.

Funding
This work was supported by the National Natural Science Foundation of China (No. 82270111 and 81973991 to WLM; No. 82070066 and 82270075 to HY).

Data availability
No datasets were generated or analysed during the current study.

Declarations

Ethical approval
The study protocol was approved by the Ethics Committee of Union Hospital (ID: S1220), Tongji Medical College, Huazhong University of Science and Technology, Wuhan, China. Informed consent was obtained from all control subjects and patients with DM. This part of the study was conducted according to the Declaration of Helsinki.

Consent for publication
All authors have read and agreed with the submission of the manuscript. This manuscript has not been published or presented elsewhere in part or in entirety.

Competing interests
The authors declare no competing interests.

Author details
[1]Department of Respiratory and Critical Care Medicine, Union Hospital, Tongji Medical College, Huazhong University of Science and Technology, Wuhan 430022, China
[2]Department of Pathophysiology, School of Basic Medicine, Tongji Medical College, Huazhong University of Science and Technology, Wuhan 430030, China
[3]Department of Rheumatology and Immunology, Union Hospital, Tongji Medical College, Huazhong University of Science and Technology, Wuhan 430022, China
[4]Key Laboratory of Respiratory Diseases, National Health Commission of China, Wuhan 430030, China
[5]Tongji Medical College, Union Hospital, Huazhong University of Science and Technology, 1277 JieFang Avenue, Wuhan 430022, China
[6]Basic School of Medicine, Tongji Medical College, Huazhong University of Science and Technology, 13 Hang Kong Road, Wuhan 430030, China

Received: 16 November 2024 / Accepted: 15 March 2025
Published online: 23 March 2025

References

1. Mariampillai K, Granger B, Amelin D, Guiguet M, Hachulla E, Maurier F, et al. Development of a new classification system for idiopathic inflammatory myopathies based on clinical manifestations and Myositis-Specific autoantibodies. JAMA Neurol. 2018;75(12):1528–37.
2. Meyer A, Meyer N, Schaeffer M, Gottenberg JE, Geny B, Sibilia J. Incidence and prevalence of inflammatory myopathies: a systematic review. Rheumatology (Oxford). 2015;54(1):50–63.
3. Sun KY, Fan Y, Wang YX, Zhong YJ, Wang GF. Prevalence of interstitial lung disease in polymyositis and dermatomyositis: A meta-analysis from 2000 to 2020. Semin Arthritis Rheum. 2021;51(1):175–91.
4. Chen Z, Hu W, Wang Y, Guo Z, Sun L, Kuwana M. Distinct profiles of myositis-specific autoantibodies in Chinese and Japanese patients with polymyositis/dermatomyositis. Clin Rheumatol. 2015;34(9):1627–31.
5. Lian X, Zou J, Guo Q, Chen S, Lu L, Wang R, et al. Mortality risk prediction in amyopathic dermatomyositis associated with interstitial lung disease: the FLAIR model. Chest. 2020;158(4):1535–45.
6. Shakshouk H, Deschaine MA, Wetter DA, Drage LA, Ernste FC, Gibson LE, et al. Do histopathological features correlate with systemic manifestations in dermatomyositis? Analysis of 42 skin biopsy specimens from 22 patients. J Cutan Pathol. 2022;49(5):442–7.
7. Fiorentino D, Chung L, Zwerner J, Rosen A, Casciola-Rosen L. The mucocutaneous and systemic phenotype of dermatomyositis patients with antibodies to MDA5 (CADM-140): a retrospective study. J Am Acad Dermatol. 2011;65(1):25–34.
8. Shakshouk H, Deschaine MA, Wetter DA, Drage LA, Ernste FC, Lehman JS. Clinical and histopathological features of adult patients with dermatomyositis and melanoma differentiation associated-5 autoantibody seropositivity status, as determined by commercially available testing: a retrospective, single-institution comparative cohort study. Clin Exp Dermatol. 2022;47(2):282–8.
9. Ahmad S, Mu X, Yang F, Greenwald E, Park JW, Jacob E, et al. Breaching Self-Tolerance to Alu duplex RNA underlies MDA5-Mediated inflammation. Cell. 2018;172(4):797–e81013.
10. Liddicoat BJ, Piskol R, Chalk AM, Ramaswami G, Higuchi M, Hartner JC, et al. RNA editing by ADAR1 prevents MDA5 sensing of endogenous DsRNA as nonself. Science. 2015;349(6252):1115–11120.
11. Dias Junior AG, Sampaio NG, Rehwinkel J. A balancing act: MDA5 in antiviral immunity and autoinflammation. Trends Microbiol. 2019;27(1):75–85.
12. Yin X, Riva L, Pu Y, Martin-Sancho L, Kanamune J, Yamamoto Y, et al. MDA5 governs the innate immune response to SARS-CoV-2 in lung epithelial cells. Cell Rep. 2021;34(2):108628.
13. Lion A, Esnault E, Kut E, Guillory V, Trapp-Fragnet L, Soubies SM, et al. Chicken endothelial cells are highly responsive to viral innate immune stimuli and are susceptible to infections with various avian pathogens. Avian Pathol. 2019;48(2):121–34.
14. Nombel A, Fabien N, Coutant F. Dermatomyositis with Anti-MDA5 antibodies: bioclinical features, pathogenesis and emerging therapies. Front Immunol. 2021;12:773352.
15. Zahn S, Barchet W, Rehkämper C, Hornung T, Bieber T, Tüting T, et al. Enhanced skin expression of melanoma differentiation-associated gene 5 (MDA5) in dermatomyositis and related autoimmune diseases. J Am Acad Dermatol. 2011;64(5):988–9.
16. Ichimura Y, Konishi R, Shobo M, Tanaka R, Kubota N, Kayama H, et al. Autoimmunity against melanoma differentiation-associated gene 5 induces interstitial lung disease mimicking dermatomyositis in mice. Proc Natl Acad Sci U S A. 2024;121(16):e2313070121.
17. Oakes SA, Papa FR. The role of Endoplasmic reticulum stress in human pathology. Annu Rev Pathol. 2015;10:173–94.

18. Braakman I, Bulleid NJ. Protein folding and modification in the mammalian Endoplasmic reticulum. Annu Rev Biochem. 2011;80(1):71–99.
19. Hetz C. The unfolded protein response: controlling cell fate decisions under Er stress and beyond. Nat Rev Mol Cell Biol. 2012;13(2):89–102.
20. Bode RK, Klein-Gitelman MS, Miller ML, Lechman TS, Pachman LM. Disease activity score for children with juvenile dermatomyositis: reliability and validity evidence. Arthritis Rheum. 2003;49(1):7–15.
21. Smith RL, Sundberg J, Shamiyah E, Dyer A, Pachman LM. Skin involvement in juvenile dermatomyositis is associated with loss of end row nailfold capillary loops. J Rheumatol. 2004;31(8):1644–9. PMID: 15290747.
22. Cao X, Fang X, Guo M, Li X, He Y, Xie M, et al. TRB3 mediates vascular remodeling by activating the MAPK signaling pathway in hypoxic pulmonary hypertension. Respir Res. 2021;22(1):312.
23. Cao X, Fang X, Malik WS, He Y, Li X, Xie M, et al. TRB3 interacts with ERK and JNK and contributes to the proliferation, apoptosis, and migration of lung adenocarcinoma cells. J Cell Physiol. 2020;235(1):538–47.
24. Almanza A, Carlesso A, Chintha C, Creedican S, Doultsinos D, Leuzzi B, et al. Endoplasmic reticulum stress signalling - from basic mechanisms to clinical applications. FEBS J. 2019;286(2):241–78.
25. Abe Y, Kusaoi M, Tada K, Yamaji K, Tamura N. Successful treatment of anti-MDA5 antibody-positive refractory interstitial lung disease with plasma exchange therapy. Rheumatology (Oxford). 2020;59(4):767–71.
26. Iwakoshi NN, Lee AH, Vallabhajosyula P, Otipoby KL, Rajewsky K, Glimcher LH. Plasma cell differentiation and the unfolded protein response intersect at the transcription factor XBP-1. Nat Immunol. 2003;4(4):321–9.
27. Gao Y, Sartori DJ, Li C, Yu QC, Kushner JA, Simon MC, et al. PERK is required in the adult pancreas and is essential for maintenance of glucose homeostasis. Mol Cell Biol. 2012;32(24):5129–39.
28. Scharer CD, Patterson DG, Mi T, Price MJ, Hicks SL, Boss JM. Antibody-secreting cell destiny emerges during the initial stages of B-cell activation. Nat Commun. 2020;11(1):3989.
29. Yu WK, Chen WC, Su VY, Shen HC, Wu HH, Chen H, et al. Nintedanib inhibits endothelial mesenchymal transition in Bleomycin-Induced pulmonary fibrosis via focal adhesion kinase activity reduction. Int J Mol Sci. 2022;23(15):8193.
30. Yacoub Wasef SZ, Robinson KA, Berkaw MN, Buse MG. Glucose, dexamethasone, and the unfolded protein response regulate TRB3 mRNA expression in 3T3-L1 adipocytes and L6 myotubes. Am J Physiol Endocrinol Metab. 2006;291(6):E1274–80.
31. Cheng W, Mi L, Tang J, Yu W. Expression of TRB3 promotes epithelial mesenchymal transition of MLE 12 murine alveolar type II epithelial cells through the TGF β1/Smad3 signaling pathway. Mol Med Rep. 2019;19(4):2869–75.
32. Yu W, Mi L, Wang F. Effect of the alteration of tribbles homologue 3 expression on epithelial–mesenchymal transition of transforming growth factor β1–induced mouse alveolar epithelial cells through the Wnt/β–catenin signaling pathway. Mol Med Rep. 2020;21(2):615–22.
33. Zheng D, Guo J, Liang Z, Jin Y, Ding Y, Liu J, et al. Supramolecular nanofibers ameliorate Bleomycin-Induced pulmonary fibrosis by restoring autophagy. Adv Sci (Weinh). 2024;11(28):e2401327.
34. Kato H, Takeuchi O, Sato S, Yoneyama M, Yamamoto M, Matsui K, et al. Differential roles of MDA5 and RIG-I helicases in the recognition of RNA viruses. Nature. 2006;441(7089):101–5.
35. Wu B, Peisley A, Richards C, Yao H, Zeng X, Lin C, et al. Structural basis for DsRNA recognition, filament formation, and antiviral signal activation by MDA5. Cell. 2013;152(1–2):276–89.
36. Liu Y, Feng S, Liu X, Tang Y, Li X, Luo C, et al. IFN-beta and EIF2AK2 are potential biomarkers for interstitial lung disease in anti-MDA5 positive dermatomyositis. Rheumatology (Oxford). 2023;62(11):3724–31.
37. Liao AP, Salajegheh M, Nazareno R, Kagan JC, Jubin RG, Greenberg SA. Interferon B is associated with type 1 interferon-inducible gene expression in dermatomyositis. Ann Rheum Dis. 2011;70(5):831–6.
38. Li L, Chen S, Wen X, Wang Q, Lv G, Li J, et al. Positive association between ANKRD55 polymorphism 7731626 and dermatomyositis/polymyositis with interstitial lung disease in Chinese Han population. Biomed Res Int. 2017;2017:2905987.
39. Song J, Kim D, Hong J, Kim GW, Jung J, Park S, et al. Meta-Analysis of polymyositis and dermatomyositis microarray data reveals novel genetic biomarkers. Genes (Basel). 2019;10(11):864.
40. Kochi Y, Kamatani Y, Kondo Y, Suzuki A, Kawakami E, Hiwa R, et al. Splicing variant of WDFY4 augments MDA5 signalling and the risk of clinically amyopathic dermatomyositis. Ann Rheum Dis. 2018;77(4):602–11.
41. Zhang CE, Li Y, Wang ZX, Gao JP, Zhang XG, Zuo XB, et al. Variation at HLA-DPB1 is associated with dermatomyositis in Chinese population. J Dermatol. 2016;43(11):1307–13.
42. Sun X, Sun L, Zhao Y, Li Y, Lin W, Chen D, et al. MAVS maintains mitochondrial homeostasis via autophagy. Cell Discov. 2016;2:16024.
43. Xue M, Wang W, He H, Li L, Zhang X, Shi H, et al. Different mechanisms are utilized by coronavirus transmissible gastroenteritis virus to regulate interferon lambda 1 and interferon lambda 3 production. J Virol. 2022;96(24):e0138822.
44. Waldman R, DeWane ME, Lu J, Dermatomyositis. Diagnosis and treatment. J Am Acad Dermatol. 2020;82(2):283–96.
45. Chen X, Jiang W, Jin Q, Lin S, Zhang L, Peng Q, et al. Nintedanib could potentially lead to improvements in anti-melanoma differentiation-associated 5 dermatomyositis-associated interstitial lung disease. Clin Exp Rheumatol. 2024;42(2):386–93.
46. Lian X, Ye Y, Zou J, Wu C, Ye S, Guo Q, et al. Longitudinal study of patients with antimelanoma differentiation-associated gene 5 antibody-positive dermatomyositis-associated interstitial lung disease. Rheumatology (Oxford). 2023;62(5):1910–9.
47. Lundberg IE, Tjärnlund A, Bottai M, Werth VP, Pilkington C, de Visser M, International Myositis Classification Criteria Project Consortium, the Euromyositis Register, and the Juvenile Dermatomyositis Cohort Biomarker Study and Repository (UK and Ireland), et al. 2017 European league against rheumatism/american college of rheumatology classification criteria for adult and juvenile idiopathic inflammatory myopathies and their major subgroups. Arthritis Rheumatol. 2017;69(12):2271–82.
48. Wang A, Morgan GA, Paller AS, Pachman LM. Skin disease is more recalcitrant than muscle disease: A long-term prospective study of 184 children with juvenile dermatomyositis. J Am Acad Dermatol. 2021;84(6):1610–8.
49. Schwartz T, Sanner H, Gjesdal O, Flatø B, Sjaastad I. In juvenile dermatomyositis, cardiac systolic dysfunction is present after long-term follow-up and is predicted by sustained early skin activity. Ann Rheum Dis. 2014;73(10):1805–10.

Publisher's note

Springer Nature remains neutral with regard to jurisdictional claims in published maps and institutional affiliations.